Hindawi
Discrete Dynamics in Nature and Society
Volume 2023, Article ID 1183764, 21 pages
https://doi.org/10.1155/2023/1183764

Research Article

Multivisit Drone-Vehicle Routing Problem with Simultaneous Pickup and Delivery considering No-Fly Zones

Yan-Qiu Liu,[1] Jing Han ,[1] Ying Zhang,[1] Yan Li,[2] and Tao Jiang[1]

[1]*School of Management, Shenyang University of Technology, Shenyang 110870, China*
[2]*School of Transportation and Logistics Engineering, Wuhan University of Technology, Wuhan 430063, China*

Correspondence should be addressed to Jing Han; hanjing@smail.sut.edu.cn

Received 17 April 2023; Revised 16 July 2023; Accepted 28 July 2023; Published 22 August 2023

Academic Editor: Hector Vazquez-Leal

The employment of drones for the distribution of goods represents a significant avenue for addressing logistical challenges at the end of the supply chain. The truck-drone cooperative delivery model overcomes drone limitations such as limited capacity and endurance and has emerged as a crucial mode of drone participation in logistics delivery. This delivery model effectively reduces delivery costs and shortens delivery times. Herein, we examine a variant of the truck-drone routing problem, which encompasses the strategic deployment and routing of multiple fleets of trucks, each equipped with an auxiliary drone. The objective is to fulfill all the pickup and delivery demands of a designated customer base while minimizing the overall route cost. Within this problem domain, drones are authorized to serve multiple customers within their capacity and endurance limits, providing both pickup and delivery services during each trip. However, the utilization of drones for servicing all customers is impeded by the existence of no-fly zones that have been implemented in numerous cities worldwide. These prescribed no-fly zones cause significant challenges when attempting to optimize the routing of truck-drone operations. Thus, this study constructs a mixed integer linear programming (MILP) model for the path optimization problem of joint service of trucks and drones considering no-fly zones and simultaneous pickup and delivery. Given the intricacy of the MILP model, we propose a two-stage heuristic algorithm based on a simulated annealing approach, combined with strategies for rectifying infeasible solutions and expediting algorithmic processes. During the phase of computational experimentation, we explore the advantages derived from enabling drones to serve multiple customers and assess the effectiveness of the proposed model and two-stage heuristic algorithm. Finally, sensitivity analysis is conducted on two key parameters.

1. Introduction

For a long time, the "last mile" has consistently been the bottleneck in the efficiency of the distribution process. Improving the operational efficiency of the "last mile" is crucial to logistics companies and even society. Currently, in the "last-mile" distribution, trucks often have low distribution efficiency due to urban traffic congestion or rugged mountain roads, which pose significant challenges to logistics companies. However, the application of drones in the distribution field has the advantages of not being affected by ground obstacles, fast delivery, and low cost; hence, it has attracted increasing attention from the industry and research scholars. Although the load capacity of drones is small and battery technology cannot support long-range delivery, the joint delivery of trucks (ground vehicles) and drones can form a novel and efficient delivery mode [1] which has led to research on the drone-vehicle routing problem (DVRP). Furthermore, introducing pickup services into this novel combination model could offer a practical and promising last-mile solution, given the growing demand and practical importance of reverse logistics.

The drone-vehicle routing problem with simultaneous pickup and delivery (DVRPSPD) is a complex route planning problem. This problem aims to meet the pickup and delivery requirements of a set of customers while minimizing the route cost. The characteristics of this problem are as follows. First, joint delivery by trucks and drones is considered. The truck fleets start and end at the depot, and the drones are launched and retrieved from the depot or the

truck they are transported to. The trucks are responsible for long-distance pickup and delivery tasks, while the drones handle the same short-distance tasks. This service method can greatly reduce labor and time costs while enhancing service efficiency. Additionally, it considers simultaneous pickup and delivery for meeting the customer needs. Unlike traditional parcel delivery, this method enables trucks and drones to provide pickup and delivery services during the same trip, which greatly reduces delivery time and improves delivery efficiency.

In 2013, Amazon's drone delivery plan marked the earliest instance of drone involvement in delivery services. Three years later, the Prime Air drone by Amazon successfully delivered its first order. In subsequent tests, drone delivery services have shown to be effective in certain scenarios. For instance, in Shenzhen, China, drones have been utilized to deliver goods and food from stores or restaurants to customers, offering residents near business districts a novel "3 km 15 min" service experience in response to the boom in instant retail [2]. Furthermore, some companies began exploring synchronous collaboration systems that combine trucks and drones. Mercedes–Benz's Vision Van, for instance, includes a fully automated cargo space and two rotor drones for autonomous delivery.

While the purpose of these tests was to address the technical hindrances associated with drone delivery services, certain researchers have delved into the issue from an operational standpoint. For example, Kim et al. [3] placed emphasis on the planning of drone-assisted healthcare services, which involves drones being utilized for delivering medicine to patients and collecting samples such as blood or urine tests. Ham [4] extended the parallel drone scheduling traveling salesman problem (PDSTSP), considering the drone's cargo and pickup functions. This means that the drone can either return to the depot after completing a delivery or directly move to another customer to pick up goods. Wikarek et al. [5] also explored the capacitated vehicle routing problem with drones, which involves drones delivering packages to customers while also retrieving packages from them using multiple mobile depots to launch and retrieve drones. However, their study only used drones for pickup and delivery independently rather than in synchronous conjunction with trucks. Current research on combinatorial problems primarily focuses on delivery services [6–13]. In light of this, Zhang and Li [14] introduced the pickup and delivery service into the collaborative distribution system of trucks and drones to maximize drone usage. However, their study does not take into account the capacity constraint of the truck and restricts the launch and retrieve node of the drone to be the same node, which simplifies the problem and increases the waiting time. Meng et al. [15] broke this limitation and extended the problem to the vehicle routing problem with simultaneous pickup and delivery (VRPSPD) for the study.

Despite the advantages of using drones for delivery and pickup operations, implementing such services is still in its infancy and limited to specific scenarios. There are some obstacles to wider adoption, as numerous cities have instituted no-fly zones to ensure the safety of drone deliveries and protect the public interest. These no-fly zones restrict drones from entering sensitive areas, such as airports, nuclear power plants, and government buildings, to avoid potential security threats, infringement of the legal rights of others, and interference with the normal operation of public facilities. In the joint distribution path planning problem of drones and trucks, the existence of no-fly zones limits the movement range and path selection of drones and increases the complexity and difficulty of the problem, which is suitable for the actual drone delivery scene. Therefore, the existence of no-fly zones in the joint delivery of trucks and drones is necessary.

To increase the utilization rate of drones, some technically feasible operations can be considered, such as allowing drones to carry multiple packages per trip and providing simultaneous pickup and delivery services, not just delivery, which can increase the utility of the drone. Currently, there is no literature that considers the existence of no-fly zones in the study of the DVRPSPD. Therefore, this study considers the impact of no-fly zones on path planning based on the DVRPSPD and allows drones to provide pickup and delivery services for multiple customers within their capacity and endurance. This problem is known as the multivisits drone-vehicle routing problem with simultaneous pickup and delivery considering no-fly zones (MDVRPSPDNF). We built a discrete optimization model with the goal of minimizing the route cost, aiming to provide theoretical support for improving the logistics company's response to customers' various needs and the normal delivery of drones. Furthermore, we propose a two-stage heuristic algorithm based on the simulated annealing (SA) algorithm, which includes a path encoding method that can represent the branch structure, an adjustment method for infeasible solutions, and an algorithm acceleration strategy. This algorithm is fast and effective in solving the MDVRPSPDNF problem. Finally, we observe through computational experiments that a combined truck-drone system allowing multiple visits per trip saves significant delivery costs. The results of these numerical experiments indicate that logistics enterprises would not only achieve cost reduction and increase efficiency from route optimization but also consider the rationality of flexible and effective distribution vehicles and resource allocation.

2. Related Literature

This section provides a synopsis of the pertinent literature that previously explored concepts in relation to the research presented in this study. For a more extensive summary and survey, we direct the reader to studies conducted by Otto et al. [16], Khoufi et al. [17], Macrina et al. [18], and Madani and Ndiaye [19].

Murray and Chu [6] initially proposed the flying sidekick traveling salesman problem (FSTSP), which serves as a cornerstone for the joint truck-drone route optimization problem, garnering considerable attention from both industry and academia. In this problem, a truck carries a drone for delivery purposes, with each drone flight serving only one customer. Based on FSTSP, Ha et al. [7] solved the

FSTSP problem by modifying the objective function from minimizing delivery time to minimizing delivery costs. They proposed two heuristic methods—TSP-local search (TSP-LS) and greedy randomized adaptive search procedure (GRASP)—to address this issue. Agatz et al. [8] proposed the traveling salesman problem with drone (TSPD), where they set the drone retrieve node limit and the drone launch node limit to the same node, and designed a hybrid algorithm that combines local search and dynamic programming to solve the problem. Later, Mario et al. [20] explored the possibility of along-route operations in the TSPD, allowing the drone to serve a broader area. Chang and Lee [21] highlighted the importance of finding a better route based on the TSPD to achieve a larger drone delivery area. They established a nonlinear planning model and demonstrated its effectiveness. Yurek and Ozmutlu [22] proposed a decomposition-based iterative algorithm for moderately sized TSPD problems. Kim and Moon [23] introduced drone stations to the TSPD, creating the traveling salesman problem with drone stations. Wang et al. [24] examined the TSPD from a manager's perspective, with biobjectives of operating cost and completion time, and proposed an improved nondominated sorting genetic algorithm to solve the problem. Additionally, several studies focused on exploring precise methods for the FSTSP/TSPD [25–28] and heuristic algorithms [29, 30].

Kitjacharoenchai et al. [9] extended the FSTSP problem, proposing a new variant of a truck carrying multiple drones. To this end, they established a mixed integer programming (MIP) model and heuristic algorithm. Murray and Raj [31] conducted an in-depth study of the multiple flying sidekicks traveling salesman problem (MFSTSP), considering the energy consumption model of drones with respect to the package weight, speed, and operation time. They proposed a three-stage iterative heuristic algorithm that can handle up to 100 customer instances. Furthermore, Peng et al. [32] proposed a truck-assisted multidrone package delivery method and provided a hybrid genetic algorithm to solve the problem. Freitas and Penna [33] proposed a novel MFSTSP for parcel delivery services using parking-assisted truck-drones as an alternative to FSTSP. Dell'Amico et al. [34], Gavani et al. [35], Lu et al. [36], and Tinic et al. [37] studied exact and heuristic algorithms to solve MFSTSP problems.

Gonzalez et al. [10] expanded on the FSTSP problem, also known as the truck-drone team logistics problem, by considering the number of customers a drone visits during a single trip. This approach allows drones to visit multiple customers, which reduces delivery costs. Luo et al. [38] delved further into the issue with their study of the multivisit traveling salesman problem with multidrones, considering drone energy consumption factors such as flight time, self-weight, and payload. They proposed a multistart tabu search algorithm to solve the problem for up to 100 customers. Windras Mara et al. [39] introduced a new mathematical formulation and a heuristic algorithm based on adaptive large-scale neighborhood search (ALNS) techniques to optimize the route for combined systems. Mahmoudi and Eshghi [40] explored the energy-constrained multivisit traveling salesman problem for multiple drones at noncustomer rendezvous locations, providing a mathematical model and heuristic algorithm for large-scale examples.

Wang et al. [11] expanded the single-truck fleet problem to encompass multiple trucks and designated it as the vehicle routing problem with drone (VRPD) to better fit the practical distribution scenarios of enterprises. Masmoudi et al. [12] analyzed the operational expenses of VRPD and devised an ALNS algorithm to handle issues with up to 250 customers. Ulmer and Thomas [13] centered their VRPD research on the same-day delivery. Wang and Sheu [41], Tamke and Buscher [42], and Zhen et al. [43] each employed exact algorithms to solve the VRPD model. Euchi and Sadok [44] proposed a hybrid genetic sweeping algorithm for addressing the VRPD problem involving up to 200 customers. Lei et al. [45] adopted a novel dynamic artificial bee colony algorithm to minimize overall operating costs for the VRPD. Schermer et al. [46] broadened the VRPD to include multiple drones per truck to serve all customers. Masmoudi et al. [12] extended the VRPD to a fleet of drones equipped with payload bays for serving more customers during a single trip. In Kuo et al. [47] study, a biobjective mathematical model of the VRPD was established to minimize delivery completion time and carbon emissions. They proposed a nondominated sorting-based genetic algorithm to solve this problem.

Kuo et al. [48] explored the VRPD with customer time windows by minimizing travel costs in their study that integrates multiple factors. They developed a variable neighborhood search algorithm to solve a fifty-customer problem. Dayarian et al. [49] proposed a delivery service based on the VRPD, where trucks meet the needs of customers who placed orders, while drones fulfill newly emerging dynamic needs. Kim et al. [3] focused on drone-assisted medical services that deliver medicine to patients and retrieve test kits such as blood or urine samples. Ham [4] extended the PDSTSP to include the delivery and pickup of the drone. Wikarek et al. [5] studied the capacity vehicle routing problem with drones that not only deliver but also accept packages from customers and used several mobile depots for drone launch and retrieval. Lu et al. [50] performed an advantageous study on the cooperative distribution system of trucks and drones in the multiobjective humanitarian routing problem. In their study, customers are defined as demand points or replenishment points. In contrast, in Zhang and Li's study [14], the customer is both a demand point and a replenishment point, and it is restricted that the launch and retrieve node of the drone must be the same. But their study did not take into account the capacity constraints of trucks. However, Meng et al. [15] allowed the launch and retrieve node of the drone to be different and extended this problem to the VRPSPD for research. Jeong et al. [51] considered two critical practical issues, namely, the impact of package weight on drone energy consumption and no-fly zones, and extended the previous vehicle routing model to hybrid delivery systems.

However, there are no VRPD studies that simultaneously addressed pickup and delivery in no-fly zones. Numerous cities in the world have designated no-fly zones, preventing drones from visiting customers within them. This imposes

greater demands and obstacles on the route planning of both trucks and drones. Our approach allows each drone to serve multiple customers on a single trip, making joint route optimization between trucks and drones more practical. Hence, the flexibility of the MDVRPSPDNF yields new practical pickup and delivery models. Recent research results in this field are summarized in Table 1.

T represents the number of trucks, D represents the number of drones carried on each truck or the number of drones when serving customers independently with the truck, and m is the abbreviation of "Multiple." SV/MV represents the number of customers per trip (i.e., single visit or multiple visits). SPD represents whether the problem considers both demand for pickup and delivery at the same time. NF represents whether the problem considers no-fly zones. The above literature suggests that the joint distribution problem of drones and trucks can be regarded as adding drones to the VRP. Therefore, there are also numerous types of research worth learning in this regard [52, 53].

3. Model

3.1. Problem Description. We examine the scenarios of forward and reverse terminal logistics distribution in the presence of no-fly zones as the subject of research. The distribution route is optimized through the use of a cooperative distribution mode of trucks equipped with drones, as shown in Figure 1. This optimization aims to achieve wider distribution and more efficient package delivery.

The problem is defined as follows: there is a depot and multiple customers, some of whom are situated within no-fly zones. The demand and recycling volume of each customer, as well as the distance between the depot and the customers and between any two customers, is known. The depot possesses an unlimited number of homogeneous trucks and drones. A single drone can transport goods to multiple customers within its maximum loading capacity and farthest flying distance. Customers can be serviced only once by one truck or one drone. The depot dispatches several trucks and drones to transport goods to customers. The trucks are sent out from the depot, each carrying a drone, and the cargo load of the truck must not exceed its maximum loading capacity. The drone can be launched and retrieved from the depot or the truck carrying it, and it returns to the depot or its truck after delivering and receiving goods to several customers. The objective of this study is to devise a routing scheme for truck and drone services that minimize the routing cost.

MDVRPSPDNF can be described as an edge selection problem in a directed and connected network graph. Let $G = (V, A)$ be a directed graph, where $V = \{0, 1, 2, \cdots, n, n+1\}$ represents the node set, node $0, n+1$ represents the depot, the rest of the nodes represent customers, and A represents the arc set, $A = \{(i, j) \mid i \in V, j \in V, i \neq j\}$. On directed graph G, a reasonable delivery route must start from node 0 and end at node $n+1$. $C = V\backslash\{0, n+1\}$ represents the customer set, $K = \{1, 2, \cdots, k\}$ represents the set of delivery trucks, and $P = \{1, 2, \cdots, p\}$ represents the set of drone trips. $F = \{1, 2, \cdots, f\}$ refers to the gathering of customers in no-fly zones. According to the customer's demand and the weight of the recycled volume, all customers are divided into two categories: customer set C^T: $C^T = \{i \mid q_i > Q_u \| r_i > Q_u, i \in C\}$ only served by trucks, and customer set C^U: $C^U = C/C^T$ served by both trucks and drones. In set C^U, when customer i's demand q_i and recycling volume r_i do not exceed the maximum loading capacity Q_u of the drone and the travel distance after adding customer i does not exceed its farthest flying distance $D_{\max}$, drone delivery is preferred. If the above conditions are met but the route cost of using drones for distribution is higher than that of using trucks, priority is given to trucks for delivery.

The parameters and decision variables involved in the MDVRPSPDNF model are shown in Table 2.

Before building a mathematical model, some basic assumptions must be established:

(i) If either the truck or the drone arrives earlier, they must wait for the other to arrive before restarting the pickup/delivery process

(ii) Because the drone flies almost in a straight line, Euclidean distance is used for calculation; the truck is limited by the road network such that it is assumed that the distance of the truck is $d_{ij}^t = \delta \cdot d_{ij}^u$, where δ is a constant, which represents the road tortuosity

(iii) Drones are not allowed to enter no-fly zones

(iv) When the drone is delivering, the truck proceeds to the next customer node to complete the pickup and delivery needs

(v) The battery is replaced immediately after the drone meets the truck to ensure endurance in the next drone flight

(vi) The truck and drone maintain a constant speed during the delivery process

3.2. Mathematical Model. Based on the mathematical model constructed by Luo et al. [38] and combined with the specific characteristics of MDVRPSPDNF, the following model is obtained:

$$\min \quad C^t \sum_{k\in K} \sum_{i\in V} \sum_{j\in V} d_{ij}^t x_{ij}^k + C^u \sum_{k\in K} \sum_{p\in P} \sum_{i\in V} \sum_{j\in V} d_{ij}^u y_{ij}^{kp}. \quad (1)$$

Table 1: Summary of related studies.

Reference	T	D	SV/MV	SPD	NF	Objective	Method
Murray and Chu [6]	1	1	SV	No	No	Min time	MILP, heuristic
Ha et al. [7]	1	1	SV	No	No	Min cost	MILP, GRASP
Agatz et al. [8]	1	1	SV	No	No	Min time	MILP, approximation algorithm
Yurek and Ozmutlu [22]	1	1	SV	No	No	Min time	MILP, heuristic
Kitjacharoenchai et al. [9]	m	m	SV	No	No	Min time	MIP, heuristic
Raj and Murray [31]	1	m	SV	No	No	Min time	MILP, heuristic
Gonzalez et al. [10]	1	1	MV	No	No	Min time	MIP, heuristic
Luo et al. [38]	1	m	MV	No	No	Min time	MILP, heuristic
Wang et al. [11]	m	m	SV	No	No	Min time	Worst-case analysis
Masmoudi et al. [12]	m	1	MV	No	No	Min cost	MILP, ALNS
Wikarek et al. [5]	m	m	MV	No	No	Min distance	MILP, iterative algorithm
Ham [4]	m	m	MV	No	No	Min time	Constraint programming approach
Lu et al. [50]	m	m	MV	No	No	Multiobjective	MILP, heuristic
Jeong et al. [51]	1	1	SV	No	Yes	Min time	MIP, heuristic
Zhang and Li [14]	1	m	MV	Yes	No	Min distance	MIP, heuristic
Meng et al. [15]	m	m	MV	Yes	No	Min cost	MILP, two-stage heuristic algorithm
This paper	m	m	MV	Yes	Yes	Min cost	MILP, two-stage heuristic algorithm

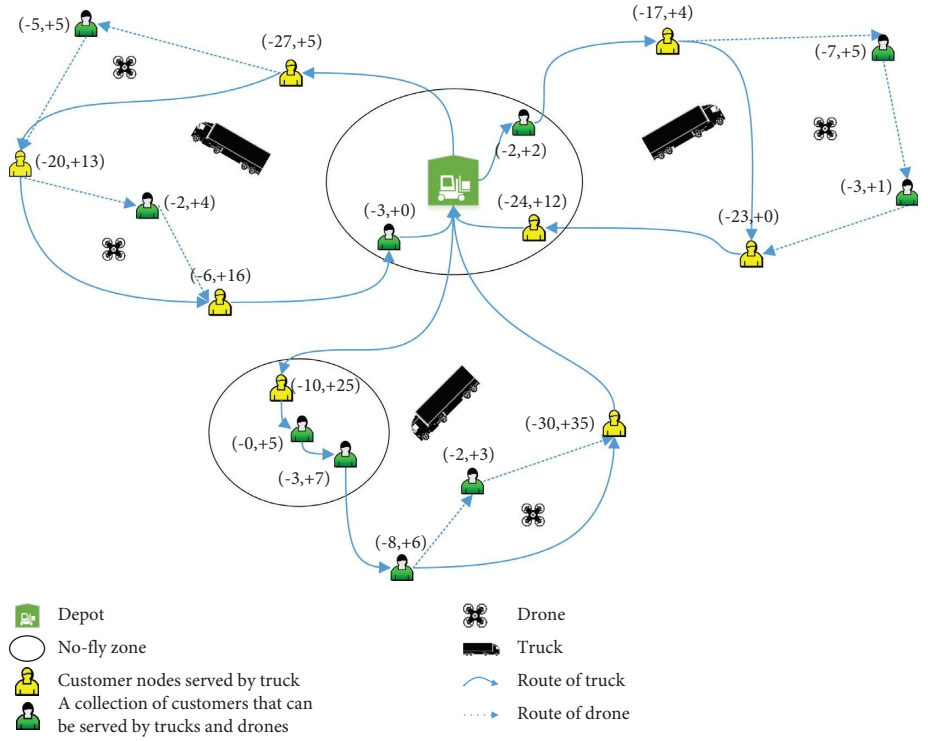

Figure 1: Example of the joint "truck-drone" distribution.

3.2.1. Route Constraints. Route constraints are given as follows:

$$\sum_{k\in K}\left(Z_i^k + \sum_{p\in P} Z_i^{kp}\right) = 1 \forall i \in C^U, \tag{2}$$

$$\sum_{k\in K} Z_i^k = 1 \forall i \in C^T, \tag{3}$$

Table 2: Model symbols and explanations.

Notation	Description
Parameters	
$D_{\max}$	Farthest flying distance of a drone
M	A large positive integer
W^u	Self-weight of drones
q_i	Demand of customer $i \in C$
r_i	Recycling volume of customer $i \in C$
Q_t/Q_u	Maximum loading capacity of trucks/drones
C^t/C^u	Unit transportation cost of trucks/drones
d_{ij}^t/d_{ij}^u	Distance between truck/drone from node $i \in V$ to node $j \in V$
Variables	
$x_{ij}^k (=1)$	Truck $k \in K$ passes through arc $(i, j) \in A$
$y_{ij}^{kp} (=1)$	Drone trip $p \in P$ carried on truck $k \in K$ passing through arc $(i, j) \in A$
$Z_i^k (=1)$	Customer $i \in C$ is served by truck $k \in K$
$Z_i^{kp} (=1)$	Customer $i \in C$ is served by drone trip $p \in P$ carried on truck $k \in K$
$h_{ikp}^S (=1)$	Customer $i \in V$ is the launch node of drone trip $p \in P$ carried on truck $k \in K$
$h_{ikp}^E (=1)$	Customer $i \in V$ is the retrieved node of drone trip $p \in P$ carried on truck $k \in K$
$g_i (=1)$	Customer $i \in C$ is in the no-fly zones
L_{0k}	Load of truck $k \in K$ when it leaves the depot
L_i^T/L_i^U	Loading capacity of truck/drone after service to customer $i \in C$
u_i/d_i	Truck/drone access sequence for node $i \in V$

$$\sum_{j \in V} x_{ij}^k = Z_i^k \forall i \in C, k \in K, i \neq j, \tag{4}$$

$$\sum_{j \in V} y_{ij}^{kp} \geq Z_i^{kp} \forall i \in C, k \in K, p \in P, i \neq j, \tag{5}$$

$$h_{ikp}^E + \sum_{j \in V} y_{ij}^{kp} = h_{ikp}^S + \sum_{j \in V} y_{ji}^{kp} \forall i \in C, k \in K, p \in P, i \neq j, \tag{6}$$

$$\sum_{j \in V} y_{ij}^{kp} \leq 1 \forall i \in V, k \in K, p \in P, i \neq j, \tag{7}$$

$$\sum_{j \in V} y_{ji}^{kp} \leq 1 \forall i \in V, k \in K, p \in P, i \neq j, \tag{8}$$

$$\sum_{j \in V} x_{ij}^k = \sum_{j \in V} x_{ji}^k \leq 1 \forall i \in V, k \in K, i \neq j, \tag{9}$$

$$\sum_{k \in K} \sum_{p \in P} y_{ij}^{kp} + \sum_{k \in K} \sum_{p \in P} y_{ji}^{kp} \leq 1 \forall (i, j) \in A, \tag{10}$$

$$\sum_{i \in C} x_{0i}^k = \sum_{i \in C} x_{i,n+1}^k \leq 1 \forall k \in K, \tag{11}$$

$$Z_i^{kp} + Z_j^{kp} \geq 1 - M\left(1 - y_{ij}^{kp}\right) \forall i \in C, j \in C, i \neq j, k \in K, p \in P, \tag{12}$$

$$h_{ikp}^S \geq 1 - M\left(2 - y_{ij}^{kp} - Z_j^{kp} + Z_i^{kp}\right) \forall i \in C, j \in C, i \neq j, k \in K, p \in P, \tag{13}$$

$$h_{jkp}^E \geq 1 - M\left(2 - y_{ij}^{kp} - Z_i^{kp} + Z_j^{kp}\right) \forall i \in C, j \in C, i \neq j, k \in K, p \in P, \tag{14}$$

$$\sum_{p \in P} h_{ikp}^S \leq M \sum_{j \in V} x_{ji}^k \forall i \in V, k \in K, i \neq j, \tag{15}$$

$$\sum_{p\in P} h_{ikp}^{E} \le M \sum_{j\in V} x_{ij}^{k} \forall i \in V, k \in K, i \ne j, \tag{16}$$

$$h_{ikp}^{S} + h_{ikp}^{E} \le 1 \forall i \in V, k \in K, p \in P, \tag{17}$$

$$\sum_{i\in V} h_{ikp}^{S} = \sum_{i\in V} h_{ikp}^{E} \le 1 \forall k \in K, p \in P, \tag{18}$$

$$\sum_{\substack{l\in V \\ l\ne 0}} x_{0l}^{k} \ge x_{ij}^{k} \forall (i,j) \in A, k \in K, \tag{19}$$

$$\sum_{i\in C} y_{0i}^{kp} + \sum_{i\in C} y_{i,n+1}^{kp} \le 1 \forall k \in K, p \in P, \tag{20}$$

$$u_i - u_j + 1 \le (n+2) \times \left(1 - x_{ij}^{k}\right) \forall k \in K, i \in V, j \in V, i \ne j, \tag{21}$$

$$d_i - d_j + 1 \le (n+2) \times \left(1 - y_{ij}^{kp}\right) \forall k \in K, p \in P, i \in V, j \in V, i \ne j. \tag{22}$$

The objective function (1) endeavors to minimize the cost of the route, which is the summation of the truck and drone route costs. Constraint (2) affirms that each customer can only receive a single service. Constraint (3) assures that customers served by trucks are exclusively served by them due to load capacity restrictions. Constraint (4) ensures that customers serviced by trucks are directly served by them. Constraint (5) ensures that customers requiring drone services are only reachable through drone trips. Every drone trip comprises an open route with a launch and retrieve node, indicating the commencement and conclusion of the trip, respectively. The launch node of a drone has solely an outdegree, and the retrieve node has solely an indegree. Constraint (6) ensures that all nodes visited by the drone trip p have a flow balance. Constraints (7) and (8) limit the total outdegree and indegree of each node. Constraint (9) maintains the flow balance of the truck and ensures that the truck can service each customer at most once. Constraint (10) necessitates that each edge is traveled at most once during a drone trip. Constraint (11) indicates that each truck can be used at most once, starting and ending from the depot. Constraint (12) mandates that for each edge visited by the drone, at least one customer must be serviced on p to prevent the drone from flying unnecessarily. Constraints (13) and (14) designate the launch and retrieve nodes for the drone's trip p. Constraints (15)–(16) require that the launch and retrieval nodes be visited by trucks. Constraint (17) guarantees that the launch and retrieve nodes of a drone trip p differ. Constraint (18) ensures that an equal number of launch and retrieve nodes are present per drone trip and that there is at most one launch node per trip. Constraint (19) indicates that each truck can only be used after leaving the depot. Constraint (20) indicates that drones are not allowed to independently complete tasks. Constraints (21) and (22) represent the subtour elimination of trucks and drones, respectively.

3.2.2. Capacity Constraints. Capacity constraints are given as follows:

$$L_{0k} = \sum_{i\in V} q_i \sum_{j\in V} x_{ij}^{k} + W^{u} + \sum_{i\in V} q_i \sum_{p\in P} \sum_{j\in V} y_{ij}^{kp} \forall k \in K, i \ne j, \tag{23}$$

$$L_{0k} \le Q_t \forall k \in K, \tag{24}$$

$$\sum_{i\in C} q_i Z_i^{kp} \le Q_u \forall k \in K, p \in P, \tag{25}$$

$$L_j^{T} \ge L_{0k} - q_j + r_j - M\left(1 - x_{0j}^{k}\right) \forall j \in C, k \in K, \tag{26}$$

$$L_j^{T} \ge L_i^{T} - q_j + r_j - M\left(1 - \sum_{k\in K} x_{ij}^{k}\right) \forall i \in C, j \in C, i \ne j, \tag{27}$$

$$L_j^U \geq \left(\sum_{l\in C} q_l Z_l^{kp}\right) - q_j + r_j - M\left(3 - y_{ij}^{kp} - Z_j^{kp} - h_{ikp}^S\right)\forall i \in C, j \in C, i \neq j, k \in K, p \in P, \tag{28}$$

$$L_j^U \geq L_i^U - q_j + r_j - M\left(3 - \sum_{p\in P} y_{ij}^{kp} - \sum_{p\in P} Z_i^{kp} - \sum_{p\in P} Z_j^{kp}\right)\forall i \in C, j \in C, i \neq j, k \in K, \tag{29}$$

$$L_j^T \leq Q_t + M\left(1 - \sum_{i\in V/\{0\}} x_{ij}^k\right)\forall j \in C, k \in K, i \neq j, \tag{30}$$

$$L_j^U \leq Q_u + M\left(1 - \sum_{i\in V/\{0\}} y_{ij}^{kp}\right)\forall j \in C, k \in K, p \in P, i \neq j. \tag{31}$$

Constraint (23) is utilized to compute the primary load of the designated truck k situated at the depot. Constraint (24) represents the maximum loading limit that the truck is capable of withstanding, while constraint (25) represents the maximum loading limit of the drone. Constraint (26) manifests as the formula for calculating the loading capacity of truck k after the initial customer has been serviced along the route. In the same vein, constraint (27) corresponds to the formula for determining the loading capacity of truck k after any other customer (excluding the first) has been serviced along the way. Similarly, constraints (28) and (29) are used to calculate the loading capacity of the drone during the trip. Constraints (30) and (31) indicate that the loading capacity of the truck and the drone after serving any customer on the route must be equal to or greater than its maximum loading capacity.

3.2.3. No-Fly Zones and Farthest Flying Distance Constraints. In the domain of logistics distribution, the incorporation of a drone can enhance distribution effectiveness and concurrently reduce costs. To ensure the safety of drone flights, a crucial approach entails the prudent delineation of obstacle avoidance routes and flight routes during the flight control of drones. Hence, it is of utmost importance to devise a rationalized flight plan and route planning while also considering the no-fly zones and the transportation requirements of drones.

The current set of no-fly zones for drones includes certain designated areas, such as airports, military bases, prisons, schools, and government properties, that permanently prohibit any sort of flying activity, alongside temporary no-fly zones that are caused by unforeseen emergencies such as forest fires. In light of this, these no-fly zones must be considered when designing the flight route, and the drone must not enter these zones.

This study delineates the no-fly zones as an area where drones are strictly prohibited from flying. Within this domain, drones are neither permitted to launch nor allowed to enter from other areas. Figure 2 highlights three distinct prohibited routes for drones traversing no-fly zones: (a) customers in no-fly zones cannot be used as the launch node of the drone; (b) customers within no-fly zones cannot be served by drones; and (c) customers in no-fly zones cannot be used as the retrieval node of the drone.

In summary, this study introduces a series of constraints to ensure the rationality and accuracy of the path planning model design and restrict the drone from passing through no-fly zones.

$$g_i = 1\forall i \in F, \tag{32}$$

$$h_{ikp}^S = 0\forall i \in F, k \in K, p \in P, \tag{33}$$

$$h_{ikp}^E = 0\forall i \in F, k \in K, p \in P, \tag{34}$$

$$y_{ij}^{kp} = 0\forall i \in F, j \in V, i \neq j, k \in K, p \in P, \tag{35}$$

$$y_{ij}^{kp} = 0\forall j \in F, i \in V, i \neq j, k \in K, p \in P, \tag{36}$$

$$\sum_{i\in V}\sum_{j\in V} d_{ij}^u y_{ij}^{kp} \leq D_{\max}\forall k \in K, p \in P, i \neq j, \tag{37}$$

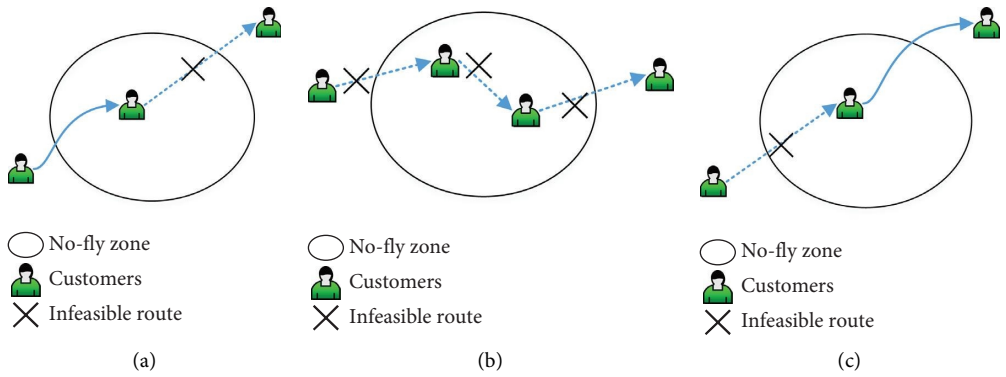

Figure 2: Schematic diagram of the route of drones prohibited from crossing the no-fly zones. (a) Prohibited launch nodes. (b) Prohibit customers served by drones. (c) Prohibited retrieve nodes.

$$x_{ij}^{k}, y_{ij}^{kp}, Z_i^k, Z_i^{kp}, h_{ikp}^{S}, h_{ikp}^{E}, g_i \in \{0,1\}, \forall i, j \in V, k \in K, p \in P, \tag{38}$$

$$L_{0k}, L_i^T, L_i^U \geq 0, \forall i \in C, k \in K, \tag{39}$$

$$u_i \geq 0, d_i \geq 0 \quad \forall i \in V. \tag{40}$$

Constraint (32) means that when customer i is in a no-fly zone, its corresponding binary variable must be 1. Constraints (33) and (34) indicate that if the drone must retrieve or launch, the retrieve/launch node must be set at a location out of the no-fly zone. Constraints (35) and (36) mean that if the path transfers from node i to node j and either node i or node j is in the no-fly zone, the decision variable y_{ij}^{kp} must be 0. Constraint (37) denotes the farthest flying distance constraint of the drone. Constraints (38) – (40) represent the value range of variables.

4. Solution Approach

As a variant of the VRP, the MDVRPSPDNF is likewise a problem that belongs to the NP-hard class. The traditional optimization method is difficult to solve; hence, we choose the SA algorithm with a simple structure that is capable of jumping out of the local optimal solution to solve it. Nevertheless, traditional SA algorithms are not capable of optimizing the truck and drone routes simultaneously. Therefore, a two-stage heuristic algorithm, based on the SA algorithm, is proposed in this study. The algorithm follows the "Route First, Cluster Second" concept. First, the problem is treated as a VRPSPD, and the SA algorithm is employed to devise the entire route. Then, customers are categorized based on their demand and recycling volume. Customers in set C^U are then excluded from the route, and drones are used to serve them. For every drone service, the minimum cost route is calculated, which satisfies the maximum loading capacity and the farthest flying distance constraints of the drone. The search process permits the drone to cater to multiple customers while adhering to the maximum loading capacity and farthest flying distance constraints. Moreover, an adjustment mechanism for infeasible solutions is devised to comply with the no-fly zone constraints. To enhance the iteration speed of the algorithm, an acceleration technique is proposed. This approach greatly reduces the complexity of the calculation problem and improves the efficiency of the algorithm search. The specific algorithm is elaborated as follows.

4.1. The First Stage: Simulated Annealing Algorithm to Solve the VRPSPD. The central idea of the SA algorithm is to obtain the optimal solution by performing several neighborhood operations on the current solution. Compared with other optimization algorithms, SA allows the acceptance of a solution that is worse than the current one with a specific probability during the search process. This attribute enables the algorithm to avoid being trapped in the local optimum. When employing the SA algorithm to solve the VRPSPD, three vital stages must be incorporated: coding and objective function, neighborhood structure, and acceptance criteria and annealing.

4.1.1. Coding and Objective Function. In this study, the depot and customers are coded in the solution simultaneously, i.e., the depot is inserted into the solution in the form of a number greater than the number n of customers. The length of the solution is $n + m - 1$, where n is the number of customers and m is the number of trucks.

Considering the constraints of loading capacity, we adopt the method of imposing penalties on routes, violating the constraints to make each segmented route meet the constraints of loading capacity. Therefore, the objective function is as follows:

$$f(s) = t(s) + \alpha c(s), \tag{41}$$

$$c(s) = \sum_{k\in K} \max\{(L_{ok} - Q_t), 0\} + \sum_{k\in K}\sum_{j\in C} \max\left\{L_j^T - Q_t - M\left(1 - \sum_{i\in V} x_{ij}^k\right)\right\}, \tag{42}$$

where s is the delivery plan, $f(s)$ is the value of the objective function, $t(s)$ is the total distance cost of the vehicle, $c(s)$ is the sum of the violations of the loading constraints when the truck leaves each node on each route, and α is the weight of the violation of the loading constraints.

4.1.2. Neighborhood Structure. This study uses a roulette wheel method to choose three neighborhood operations: the swap operation, reverse operation, and insertion operation.

Swap operation: As the name implies, this operation swaps the positions of two customers. For the existing route Route = $[r(1), \cdots, r(i), \cdots, r(j), \cdots, r(n+m-1)]$, the exchange position is selected as i and j; then, the exchanged solution is Route = $[r(1), \cdots, r(j), \cdots, r(i), \cdots, r(n+m-1)]$.

Reverse operation: A reverse operation means reversing the ordering of all customers between two locations. For the existing route Route = $[r(1), \cdots, r(i), r(i+1), \cdots, r(j-1), r(j), \cdots, r(n+m-1)]$, the reversal position is chosen as i and j; then, the solution after reversal is Route = $[r(1), \cdots, r(j), r(j-1), \cdots, r(i+1), r(i), \cdots, r(n+m-1)]$.

Insert operation: The insert operation inserts the customer selected at the first position after the customer selected at the second position. For the existing route, Route = $[r(1), \cdots, r(i), \cdots, r(j), \cdots, r(n+m-1)]$, the insertion position is chosen as i and j; then, the solution after insertion is Route = $[r(1), \cdots, r(i-1), r(i+1), \cdots, r(j), r(i), r(j+1), \cdots, r(n+m-1)]$.

4.1.3. Acceptance Criteria and Annealing. The core concept of SA is to accept a solution worse than the current solution with a certain probability. The formula for the probability of accepting a new solution is as follows:

$$P = \begin{cases} 1, & f(S_{\text{new}}) < f(S_{\text{curr}}), \\ e^{-[f(S_{\text{new}}) - f(S_{\text{curr}})]/T}, & f(S_{\text{new}}) \geq f(S_{\text{curr}}), \end{cases} \tag{43}$$

where $f(S_{\text{curr}})$ represents the objective function value of the current solution and $f(S_{\text{new}})$ represents the objective function value of the new solution.

As the number of iterations increases, the probability of acceptance must also decrease. This is because the search time must be reduced, i.e., the temperature decreases with the increase in the number of iterations, and the formula is as follows:

$$T_{\text{gen}+1} = \beta T_{\text{gen}}, \tag{44}$$

where β is the cooling factor and $0 < \beta < 1$.

4.2. The Second Stage: Routing Algorithms for Truck-Drone. The multivisit drone-vehicle routing problem for pickup and delivery conundrum encompasses three distinct decisions. The first step is to determine which customers are served by trucks and drones, respectively. The subsequent decision involves determining the order in which the truck will visit the customers. The third decision involves designating the sequence in which each drone will visit the customers as well as deciding upon launch and retrieve nodes. These nodes can either be the depot or any customer location for the truck service. Imperatively, these decisions have a consequential impact on one another and therefore must be made in tandem. The ensuing discourse delves into each of these three decisions.

4.2.1. Truck-Drone Routing Representation. The combined route for a truck and drone is depicted in Figure 3(a), along with its corresponding encoding solution is depicted in Figure 3(b). The encode comprises two components: the first part, denoted as Part 1, represents the order in which the customers are visited by the truck. This section commences and concludes with 0, which denotes the depot. The digits between two zeros indicate the customer visitation sequence for the truck service.

The second part, referred to as Part 2, represents the sequence of customers visited by the drone. The first and last digits in this section signify the launch and retrieve nodes for each drone trip, respectively. The k-th row pertains to the route taken by the k-th truck, while the p-th trip of the drone carried by the k-th truck is represented by the drone route.

To facilitate ease of handling, solutions are presented as multidimensional arrays. Given n customers, k trucks, and k drones, a single drone may undertake a maximum of p trips, and the solution is coded in kq dimensions. $q = \max k_p + 1$, where $\max k_p$ represents the maximum number of trips among k drones. This arrangement allows for the maximum number of trips made by the truck and drone. The decoded route shown in Figure 3(b) comprises the following: the route taken by the first truck is (0⟶1⟶3⟶4⟶0), while the first trip of the drone carried by the first truck is (1⟶2⟶3), and the second trip of the drone carried by the first truck is (4⟶5⟶6⟶0); the route taken by the second truck is (0⟶7⟶8⟶10⟶0), and the first trip of the drone carried by the second truck is (8⟶9⟶10). Evidently, the coding of multidimensional arrays lucidly demonstrates the collaborative distribution route of multiple trucks and drones. This coding methodology can also be expanded to other combinatorial optimization problems featuring branching structures.

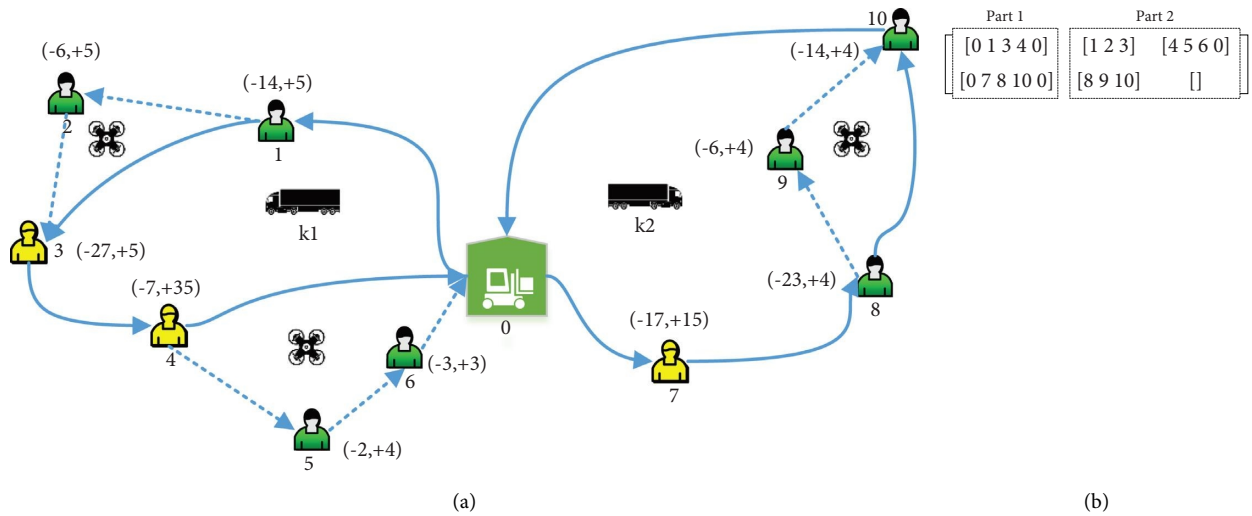

Figure 3: Representation of the joint truck-drone routing solution. (a) Routing diagram. (b) Coding.

4.2.2. Joint Truck-Drone Routing Planning. We use the pseudocode shown in Algorithm 1 (Figure 4) to plan the routing of trucks and drones. First, we classify all customers according to their demand and recycling volume, where customer set C^T is only served by trucks and customer set C^U is served by both trucks and drones. Then, the customers in set C^U are removed, served by drones, and added to drone trip $p1$. Next, we put the former node of the removed node into trip $p1$ as its launch node. Then, we determine the type of the subsequent node of the removed node. If it belongs to set C^T, it is used as the retrieval node of drone trip $p1$; if it belongs to set C^U, it is added to trip $p1$, and we continue to judge the next node type of the subsequent node until customer or depot 0 in set C^T is found. Notably, when constructing a drone path, it must meet the drone capacity and endurance. If the constraint is not met, the path is discarded. So far, a complete truck-drone routing solution has been generated.

4.2.3. Infeasible Solution Adjustment Strategy. The aforementioned procedures enable retrieval of the routes taken by both the truck and the drone; however, the no-fly zone constraint is not considered. Hereafter, a strategy for adjusting the infeasible solution with regard to the no-fly zones is presented herein. The specific strategy is as follows: if the customer who uses the drone service is in the no-fly zone, the customer will be added to the place where the path cost is the lowest in the carrier truck path of the drone; if the launch/retrieve node is in the no-fly zones, the customers served by the drone in the drone trip are added to the truck route or other drone trips. All cases are compared, and the route with the lowest route cost increment is chosen. Figures 5(a) and 5(b) illustrate a visual representation of this procedure.

4.2.4. Algorithm Acceleration Strategy. To improve the iteration speed of the algorithm, the following acceleration strategy is proposed to search for the optimal solution. When searching for drone service customers, it is beneficial to maximize the effectiveness of drones by considering the drone loading critical value, driving capacity critical value, and whether it can continue to serve the following customer node. In Figure 6, the drone flies from node A to the nearest customer B when the capacity and range allow it. When customer B has been served, the capacity and endurance reach a critical node. How to determine whether to continue serving customer C becomes a key question. This study proposes conditions for selecting vehicle models, to avoid the algorithm searching for many nonfeasible solutions. Table 3 lists the selection criteria. If the conditions are met, the drone proceeds to serve customer C and then returns to node D; otherwise, it returns to node D directly.

4.3. Algorithm Flowchart. Combining the above strategies, the two-stage heuristic algorithm process is shown in Figure 7.

5. Computational Experiments

In this section, we evaluate the effectiveness of the proposed two-stage heuristic algorithm and investigate the advantages of the DVRPSPDNF by conducting various experiments on numerical examples of different problem sizes. We first explore the effectiveness of the proposed algorithm without considering the no-fly zone. Then, we compare the performance of the proposed algorithm and mathematical model considering the no-fly zones. Finally, by testing problem instances of different scales, the advantages of the DVRPSPDNF over the truck-only service and single visit by drone are analyzed, and a sensitivity analysis is performed on two key parameters. The algorithm is implemented via Matlab 2018b, and all evaluations are conducted on a single computer with the Windows 10 operating system and an Intel(R) Core (TM) i5-10200H CPU @ 2.40 GHz processor.

Because DVRPSPDNF is a new problem, no existing benchmarks exist. Therefore, we choose the P1 data set

Algorithm 1	Truck-Drone routing planning
Input:	Solution of the first stage S_{VRPSPD};Customer demand q;Customer recycling volume r;Node distance matrix $dist$; Maximum loading capacity of a drone Q_u; The farthest flying distance of a drone $D_{\max}$; Customer set C
Output:	Solution $S_{VRPDSPD}$; Objective function value obj_s
1:	$\max\_k = length(S_{VRPSPD})$;
2:	$k = 1$; % Number of trucks
3:	while $k \le \max\_k$
4:	$S_{temp} = S_{VRPSPD}\{k\}$;
5:	$\max\_p = numel(S_{temp})/2$; % Set the maximum number of drone trips
6:	$[C^T, C^U] = classly(C, q, r, Q_u)$; % Customer classification
7:	$[S_{VRPDSPD}\{k\}, obj\_s\{k\}] = remove\_insert(S_{temp}, q, r, Q_u, dist, D_{\max}, \cdots$ $\max\_p, C^T, C^U)$; % " cluster " operations on each truck
8:	$k = k + 1$;
9:	end while
10:	$obj\_s = sum(obj\_s\{k\})$

Figure 4: Truck-drone routing planning pseudocode.

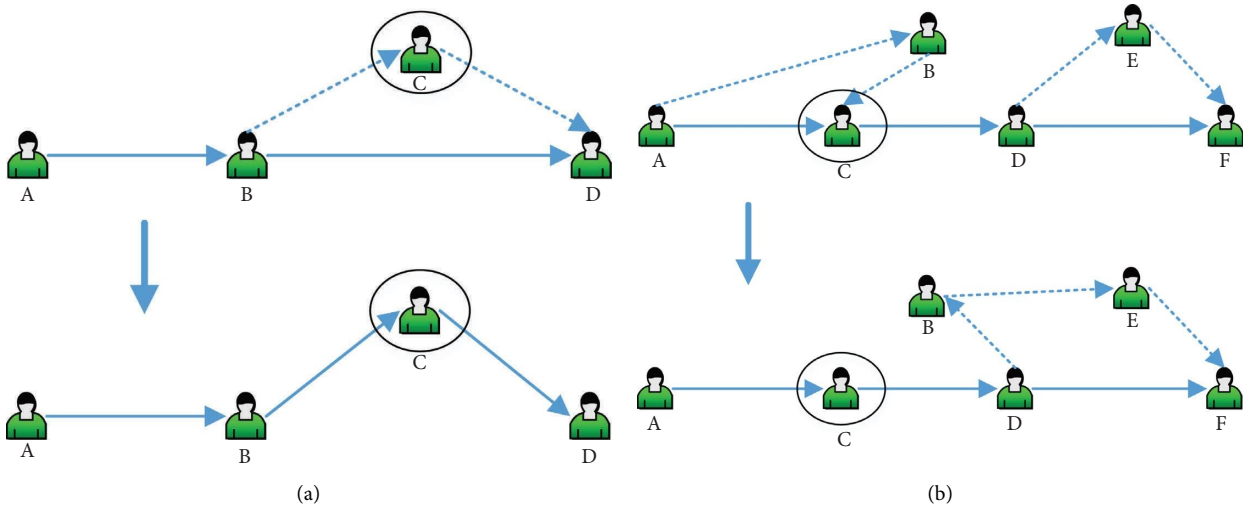

Figure 5: Schematic diagram of the adjustment strategy for a nonfeasible solution. (a) Situation where a customer served by a drone is in a no-fly zone. (b) Retrieval node of drone travel in a no-fly zone (the same is true for the launch node).

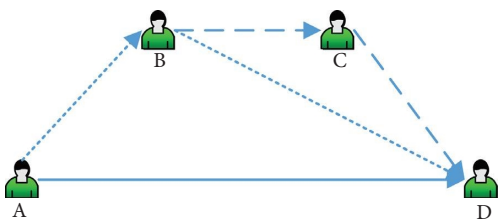

Figure 6: Schematic diagram of the tail customer judgment method.

Table 3: Selection criteria.

Analyzing condition	Result
$\begin{cases} \sum_{i\in\{b,c\}} q_i - \sum_{i\in\{b,c\}} r_i < Q_u \\ \sum_{i\in\{b,c,d\}} q_i - \sum_{i\in\{b,c,d\}} r_i < Q_u \end{cases} \&\& \begin{cases} AB + BC + CE < D_{\max} \\ AB + BC + CD + DE \le D_{\max} \end{cases}$	Accept
Other	Reject

under the VRPPD problem and the A data set under the capacitated vehicle routing problem (CVRP), which have the most similar characteristics to this study, as two types of test data. These data can be found at VRP Web (dorronsoro.es) online. Considering the actual situation and technical limitations of drones, some data must be adjusted. Thus, we adjusted the coordinate range of each example to 20 by 20 by dividing the original coordinates by five, randomly modified 86% of customers' pickup and delivery needs to be within the range of $[0, 2.3]$, and the remaining 14% of customers were adjusted in the range of $[2.3, 10]$. This is related to Amazon's statement that 86% of its packages do not exceed 2.27 kg. If the calculated number of customers selected has decimals, it is rounded down.

In numerical experiments, the numerical part of the truck- and drone-related parameters refers to published reports and current practices [54, 55]. Assuming that the maximum payload of the drone is 3 kg and the maximum flight distance is 20 km, the cost per km is approximately \$0.078. Assuming that the maximum loading capacity of the truck is 100 kg, the cost per kilometer is approximately \$0.78. The parameter settings related to the algorithm are shown in Table 4.

5.1. Comparison Experiment for Determining the Effectiveness of the Algorithm without considering No-Fly Zones. To assess the efficacy of the two-stage heuristic algorithm, we initially evaluated its performance on the P1 dataset without considering no-fly zones. We then compared the results with those obtained using the depth-first search (DFS) [56] and maximum payload-improved simulated annealing (MP-ISA) [15] in terms of objective function values. The summarized findings can be found in Table 5. Specifically, the Obj column represents the total route cost, the Time column denotes the running time, and the Gap is defined as the gap between the two-stage heuristic algorithm and DFS, calculated using formula $Gap = (Obj_{\text{Two-stage}} - Obj_{\text{DFS}})/Obj_{\text{DFS}} * 100\%$. Moreover, the Gap^0 is defined as the gap between the two-stage heuristic algorithm and MP-ISA, computed using formula $Gap^0 = (Obj_{\text{Two-stage}} - Obj_{\text{MP-ISA}})/Obj_{\text{MP-ISA}} * 100\%$.

The experimental findings demonstrate the superiority of the two-stage heuristic algorithm over DFS and MP-ISA in addressing the DVRPSPD problem. Specifically, while the DFS algorithm ensures solution quality, its search efficiency becomes limited as the problem scale expands, thereby hindering the discovery of optimal solutions. In contrast, both MP-ISA and the two-stage heuristic algorithm possess global search capabilities, enabling them to acquire reasonably good solutions within a relatively short time. However, as the problem size grows, the two-stage heuristic algorithm surpasses MP-ISA in terms of solution time and quality. On average, the two-stage heuristic algorithm achieves approximately a 4% reduction in the objective function value compared to MP-ISA. Hence, the two-stage heuristic algorithm has good adaptability and search ability when solving the vehicle routing problem with drones considering pickup and delivery, especially for situations dealing with large-scale problems.

5.2. Comparison Experiment for Determining the Effectiveness of the Algorithm considering No-Fly Zones. To verify the effectiveness of the two-stage heuristic algorithm for the no-fly zone problem, we conducted a performance comparison experiment with a mathematical model. Considering the DVRPSPDNF problem as an NP-hard problem, the model can only solve small-scale problems within a reasonable time frame. Therefore, we conducted detailed statistical analysis experiments for cases with sizes of five customers. In this example, we regarded all possible node combinations as no-fly zones, and the proportion of no-fly zones did not exceed 60%. We also conducted comparative experiments in medium and large-scale calculation examples; however, due to space limitations, we changed the selection method of the no-fly zone to randomly select several nodes to be placed in the no-fly zone. In the experiments, we used the Gurobi solver and the two-stage heuristic algorithm for testing, where the time limit of the Gurobi solver was set to 2 h. The results are summarized in Table 6, where no-fly denotes customers in no-fly zones. For the solver solution, Table 6 records the upper and lower bounds (Obj_UB, Obj_LB) of the optimal solution value obtained by Gurobi, as well as its running time (Time). For the solution of the two-stage heuristic algorithm, the table records the optimal solution value (Obj) and computation time (Time) in 20 runs and defines the gap between them as $Gap^1 = (Obj_{\text{two-stage}} - Obj_{\text{solver}})/Obj_{\text{solver}} * 100\%$.

The experimental results demonstrate that the two-stage heuristic algorithm achieves optimality for all the cases involving five customers, albeit with longer computation times when compared to Gurobi. As the number of customers increases to 10, Gurobi still manages to obtain optimal solutions within the prescribed timeframe; however, the computational time escalates considerably. While the two-stage heuristic algorithm boasts relatively shorter computation times, it does suffer from a loss of computational accuracy ranging from 6% to 7%. In the cases involving 16–20 customers, both Gurobi and the two-stage

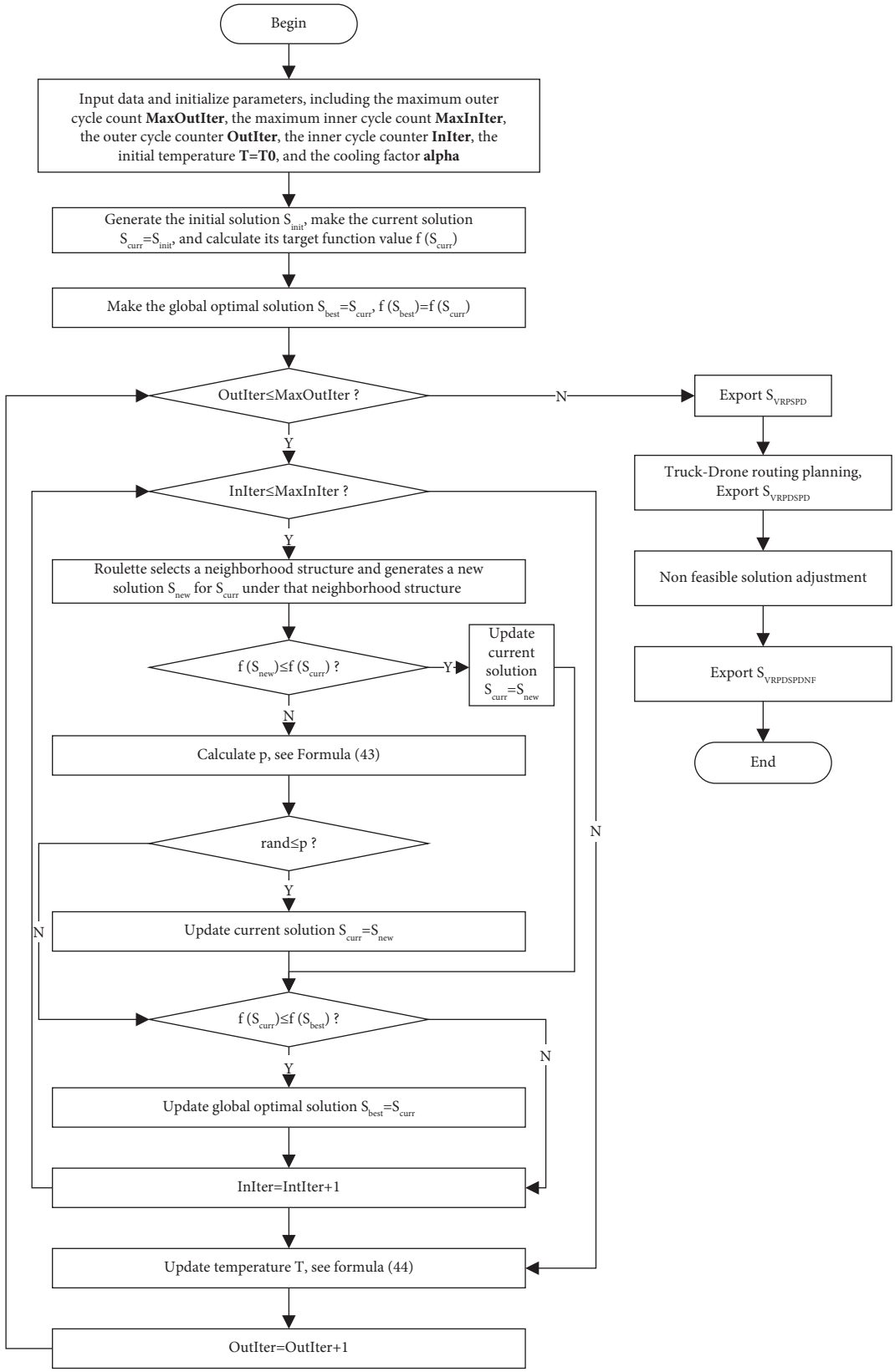

Figure 7: Flowchart of the two-stage heuristic algorithm.

Table 4: Algorithm parameters.

Parameters	Value
Penalty factor for violating load constraints	100
The maximum number of iterations of the outer loop	2000
The maximum number of iterations of the inner loop	300
The initial temperature	1000
Cooling factor	0.99
Probability of choosing an exchange operation	0.2
Probability of choosing a reversal operation	0.5
Probability of choosing an insert operation	0.3

heuristic algorithm produce approximate solutions. However, compared with the two-stage heuristic algorithm, the Gurobi solver obtains a smaller objective function value, albeit at the cost of increased solving duration. For cases involving more than 25 customers, Gurobi fails to acquire either optimal or approximate solutions, whereas the two-stage heuristic algorithm can promptly provide an approximate solution. This discrepancy arises because even a slight increment in the instance size can cause Gurobi to consume more time and memory resources. It can be seen that the solution of the solver is still unacceptably and computationally expensive; therefore, it is necessary to provide efficient heuristics for large problems. Furthermore, we found that no-fly zones have a certain impact on the total route cost by setting different numbers and locations of no-fly zones. Because no-fly zones cannot be traversed, if there are too many no-fly zones or the location layout is unreasonable, detours may be required to avoid these areas, thereby increasing the route cost. Therefore, when optimizing the route scheme in actual delivery, the location and number of no-fly zones must be considered to reduce the route cost in a targeted manner.

5.3. Comparative Analysis of Different Service Modes. To thoroughly investigate the advantages of the MDVRPSPDNF, it is imperative to conduct numerical experiments encompassing diverse service modes. Specifically, when solely considering the utilization of trucks to service customers, the scenario is referred to as the T mode. On the contrary, if the trucks operate in conjunction with drones and a single drone trip caters to only one customer, the scenario is referred to as the SV mode. Finally, when trucks and drones operate in collaboration and a single drone trip visits multiple customers, the scenario is called the MV mode.

In this section, we use three service modes to solve 10 calculation examples under dataset A and 10 calculation examples under dataset P1. In each experiment, several nodes are randomly selected to be placed in the no-fly zone, and it is assumed that the paths between other nodes do not pass through this area. The experimental results are shown in Table 7. In Table 7, Gap^2 represents the gap between MV and T, and the calculation formula is $Gap^2 = (Obj_{MV} - Obj_T)/Obj_T * 100\%$; Gap^3 represents the gap between SV and T, and the calculation formula is $Gap^3 = (Obj_{SV} - Obj_T)/Obj_T * 100\%$; Gap^4 represents the gap between MV and SV, and the calculation formula is $Gap^4 = (Obj_{\mathrm{MV}} - Obj_{\mathrm{SV}})/Obj_{SV} * 100\%$. To observe the solution in each mode more clearly, we show the path graph obtained by the two-stage heuristic algorithm in Figures 8(a)-8(c), taking the A-n32-k5 as an example.

Upon analysis of the experimental data, results indicate that in most instances, the MV service mode's route cost is approximately 13.27% lower than that of the T service mode, while the SV service mode's route cost is about 0.52% lower than that of the T service mode. This highlights that in comparison to the pure truck service model, employing a joint service of trucks and drones greatly reduces route costs. This critical conclusion must be considered when evaluating last-mile services with delivery requirements.

Furthermore, the MV service mode's route cost is about 12.83% lower than that of the SV service mode. This can be attributed to the fact that drones can service more customers in the MV mode, thereby decreasing the routing costs and the distance covered by trucks. This finding further corroborates the efficacy of the truck-mounted drone collaborative service in curtailing route costs within a brief period and the drones' ability to serve multiple customers in one trip.

Additionally, utilizing a combination of trucks and drones may not always decrease the delivery distance route. This is due to the influence of the customer base and depot location on the outcome. Specifically, if the depot is situated near the periphery of the customer region, the transport distance may not be reduced; however, some degree of the routing cost can still be saved. Conversely, if the depot is close to the center of all customers, the transportation distance and routing cost can be moderately reduced.

In summary, regardless of whether the transport distance is diminished, adopting a flexible distribution approach can effectively lower route costs, which is beneficial for enhancing customer satisfaction and aligning with current energy-saving and emission-reducing ecological principles. Simultaneously, this provides a potential solution for reducing labor costs in the future logistics sector.

5.4. Sensitivity Analysis. To further study the influence of key parameters on the experimental results, we conducted a series of tests on A-n32-k5, A-n34-k5, and A-n36-k5 examples, where we changed the drone's farthest flying distance and maximum loading capacity. In these three calculation examples, 10 levels were set for each parameter, and a total of 60 scenarios were generated. In comparison, we only change one parameter in each scenario and record the test results. First, we set the range of the farthest flight distance of the drone to start from 10 km, increase it by 10 km each time up until 10 gradients at the end of 100 km, and obtain the corresponding objective function value. The line graph is shown in Figure 9. It is not the case for all parameters that bigger values are better; for example, when the maximum loading capacity is large, it may lead to a low actual load rate. Hence, we set the maximum loading capacity of the drone to 3 kg (the drone serves one customer at a time), 12 kg (drones serve multiple customers at a time),

Table 5: Comparison of the solution results without considering no-fly zones.

Instance	Customer size	DFS		MP-ISA*		Two-stage heuristic algorithm		Gap (%)	Gap^0 (%)
		Obj ($)	Time (s)	Obj ($)	Time (s)	Obj ($)	Time (s)		
1P1	5	42.8899	0.1167	42.8899	52.7932	42.8899	25.3132	0.00	0.00
2P1	5	57.5957	0.0793	57.5957	49.8417	57.5957	25.2891	0.00	0.00
3P1	5	76.6143	0.0787	76.6143	67.1834	76.6143	25.1527	0.00	0.00
4P1	5	42.6159	0.0766	42.6159	45.9845	42.6159	25.2915	0.00	0.00
5P1	5	33.7257	0.0746	33.7257	53.7421	33.7257	25.2736	0.00	0.00
6P1	10	33.792	42554+	33.792	91.5788	33.792	27.1359	0.00	0.00
7P1	10	66.7995	45916+	66.7995	77.2730	66.7995	26.8150	0.00	0.00
8P1	10	65.5545	46132+	65.5545	89.7093	65.5545	26.4493	0.00	0.00
9P1	10	95.9622	42747+	95.9622	116.0718	95.9622	26.3039	0.00	0.00
10P1	10	53.0546	45574+	53.0546	75.3013	53.0546	26.3881	0.00	0.00
11P1	25	—	—	92.8342	111.0741	92.8342	27.9300	—	0.00
12P1	25	—	—	110.0705	107.5209	108.8239	27.8392	—	−1.13
13P1	25	—	—	84.0827	147.2939	76.1248	28.2309	—	−9.46
14P1	25	—	—	99.5778	98.6201	96.4696	28.0950	—	−3.12
15P1	25	—	—	110.4872	109.3823	114.1058	27.8189	—	3.28
16P1	50	—	—	99.4776	391.1732	99.1025	29.3064	—	−0.38
17P1	50	—	—	127.0030	446.4201	81.4187	29.3719	—	−35.89
18P1	50	—	—	92.7712	534.9052	92.7712	29.3531	—	0.00
19P1	100	—	—	150.5763	873.4260	141.0252	48.7691	—	−6.34
20P1	100	—	—	185.9799	848.1349	155.4059	31.6178	—	−16.44

The MP-ISA* algorithm is written according to the algorithm architecture in the literature [15] and is coded by using Matlab 2018b. Its objective function is to calculate the total transportation cost of trucks and drones.

Table 6: Comparison experiment for determining the effectiveness of the algorithm considering no-fly zones.

Instance	Customer size	No-fly	Solver solution			Two-stage heuristic algorithm		Gap^1 (%)
			Obj_UB ($)	Obj_LB ($)	Time (s)	Obj ($)	Time (s)	
1P1_1	5	1	25.96	25.96	1	25.96	25.3508	0.00
1P1_2	5	2	20.52	20.52	1	20.52	25.5584	0.00
1P1_3	5	3	21.76	21.76	1	21.76	25.2819	0.00
1P1_4	5	4	14.41	14.41	1	14.41	25.2415	0.00
1P1_5	5	5	14.16	14.16	1	14.16	25.0967	0.00
1P1_6	5	1, 2	27.06	27.06	1	27.06	25.2376	0.00
1P1_7	5	1, 3	31.31	31.31	1	31.31	25.2657	0.00
1P1_8	5	1, 4	26.05	26.05	1	26.05	25.0332	0.00
1P1_9	5	1, 5	25.96	25.96	1	25.96	25.0608	0.00
1P1_10	5	2, 3	25.03	25.03	1	25.03	27.5985	0.00
1P1_11	5	2, 4	20.62	20.62	1	20.62	25.0996	0.00
1P1_12	5	2, 5	20.52	20.52	1	20.52	25.0662	0.00
1P1_13	5	3, 4	22.08	22.08	1	22.08	25.1485	0.00
1P1_14	5	3, 5	21.76	21.76	1	21.76	25.0723	0.00
1P1_15	5	4, 5	20.42	20.42	1	20.42	25.5597	0.00
1P1_16	5	1, 2, 3	31.31	31.31	1	31.31	25.1711	0.00
1P1_17	5	1, 2, 4	27.15	27.15	1	27.15	25.1168	0.00
1P1_18	5	1, 2, 5	27.06	27.06	1	27.06	25.1320	0.00
1P1_19	5	1, 3, 4	31.31	31.31	1	31.31	25.2537	0.00
1P1_20	5	1, 3, 5	31.31	31.31	1	31.31	25.2396	0.00
1P1_21	5	1, 4, 5	27.07	27.07	1	27.07	25.2176	0.00
1P1_22	5	2, 3, 4	25.18	25.18	1	25.18	25.4017	0.00
1P1_23	5	2, 3, 5	25.03	25.03	1	25.03	25.0857	0.00
1P1_24	5	2, 4, 5	25.09	25.09	1	25.09	25.4050	0.00
1P1_25	5	3, 4, 5	24.77	24.77	1	24.77	25.2607	0.00
Avg.					1		25.3182	0
6P1_1	10	2	31.62	31.62	3505	33.80	30.8478	6.89
6P1_2	10	2, 5	31.72	31.72	3811	34.18	33.9215	7.76
6P1_3	10	1	31.98	31.98	3900	33.81	26.0616	5.72

Table 6: Continued.

Instance	Customer size	No-fly	Solver solution			Two-stage heuristic algorithm		Gap[1] (%)
			Obj_UB ($)	Obj_LB ($)	Time (s)	Obj ($)	Time (s)	
6P1_4	10	1, 2, 5	32.09	32.09	3242	34.28	25.9153	6.82
Avg.					3615		29.1866	6.80
11P1_1	16	2, 5	70.23*	56.81	7200	79.85	28.7801	13.70
11P1_2	16	1, 2, 5	70.33*	59.65	7200	81.15	26.9204	15.38
Avg.					7200		27.8503	14.54
11P1_3	18	2, 5	75.75*	37.98	7200	93.21	28.1936	23.05
11P1_4	18	1, 2, 5	77.08*	39.08	7200	92.58	27.0675	20.11
Avg.					7200		27.6306	21.58
11P1_5	20	2, 5	77.79*	48.12	7200	94.09	28.1038	20.95
11P1_6	20	1, 2, 5	90.81*	50.04	7200	93.35	27.9111	2.80
Avg.					7200		28.0075	11.88
11P1_7	25	2, 5, 10	—	—	—	95.49	28.3291	—
11P1_8	25	1, 5, 10, 15, 20	—	—	—	95.79	27.5383	—
Avg.							27.9337	
16P1_1	50	2, 5, 10	—	—	—	103.21	29.1527	—
16P1_2	50	1, 5, 10, 15, 20	—	—	—	103.16	28.8346	—
Avg.							28.9937	
20P1_1	100	1, 5, 15	—	—	—	171.78	31.3569	—
20P1_2	100	1, 5, 15, 25, 35	—	—	—	172.10	31.2769	—
Avg.							31.3169	

*The optimal solution cannot be obtained within a time limit of 2 h.

Table 7: Comparison of the route length and cost of different service modes.

Instance	T		SV		MV		Gap[2] (%)	Gap[3] (%)	Gap[4] (%)
	Distance (km)	Obj ($)	Distance (km)	Obj ($)	Distance (km)	Obj ($)			
A-n32-k5	738.1991	575.7953	745.819	571.2777	828.419	564.9381	−1.8856	−0.7846	−1.1097
A-n33-k5	801.5456	625.2055	825.7149	626.4847	793.8946	529.5511	−15.2997	0.2046	−15.4726
A-n33-k6	810.0986	631.8769	815.2357	605.9259	830.2485	534.8869	−15.3495	−4.1070	−11.7240
A-n34-k5	745.5779	581.5508	767.1655	582.5211	783.3361	547.3998	−5.8724	0.1668	−6.0292
A-n36-k5	765.5458	597.1257	806.9042	599.5826	757.727	498.0142	−16.5981	0.4115	−16.9399
A-n37-k5	886.4948	691.466	935.3265	687.0653	871.7529	563.1101	−18.5629	−0.6364	−18.0413
A-n37-k6	903.252	704.5366	985.2481	698.3755	846.4771	529.8001	−24.8016	−0.8745	−24.1382
A-n38-k5	929.7825	725.2303	991.0106	728.839	912.556	575.2713	−20.6774	0.4976	−21.0702
A-n39-k5	1034.5045	806.9135	1117.8947	808.0433	1216.4278	788.8451	−-2.2392	0.1400	−2.3759
A-n39-k6	768.7777	599.6466	796.249	598.4917	776.3955	439.2096	−26.7553	−0.1926	−26.6139
11P1-n25	126.494	98.6653	128.4857	97.9666	151.2918	92.725	−6.0207	−0.7082	−-5.3504
12P1-n25	145.7094	113.6533	161.9125	114.7505	198.9515	109.9613	−3.2485	0.9654	−4.1736
13P1-n25	142.3196	111.0093	144.6392	108.8874	162.599	86.701	−21.8975	−1.9115	−20.3755
14P1-n25	157.2703	122.6708	162.1433	122.0907	182.9461	110.7984	−9.6783	−0.4729	−9.2491
15P1-n25	177.2852	138.2824	179.6048	136.1605	202.3291	126.3671	−8.6166	−1.5345	−7.1925
16P1-n50	156.5053	122.0741	163.0477	122.1651	193.818	101.4892	−16.8626	0.0745	−16.9246
17P1-n50	137.9246	107.5812	137.8106	105.4266	163.1893	82.8185	−23.0177	−2.0028	−21.4444
18P1-n50	147.8966	115.3593	152.1841	115.3782	177.0224	94.7828	−17.8369	0.0164	−17.8503
19P1-n100	243.4945	189.9257	262.7141	190.4973	359.6466	178.1814	−6.1836	0.3010	−6.4651
20P1-n100	240.157	187.3224	241.7924	187.3469	369.4272	179.7767	−4.0282	0.0131	−4.0407

and 30–100 kg (starting from 30 kg and increasing by 10 kg each time up until 100 kg, for a total of eight gradients, in which the drone can provide services for any customer except for those in the no-fly zones). We obtain the corresponding objective function value, which is depicted by a line graph in Figure 10.

Figure 9 indicates that by holding other factors constant, raising the farthest flying distance of the drone will decrease the objective function value to some extent. This is due to the increased number of drone service nodes, which further reduces the overall route cost. Nevertheless, there is a lower limit on the route length and cost reduction, which is influenced by the restrictions of the drone's maximum loading capacity and no-fly zones.

Based on Figure 10, we can draw a conclusion that given other constant variables, increasing the drone's load capacity leads to a reduction in the objective function value to a certain extent, as the increased capacity allows for more

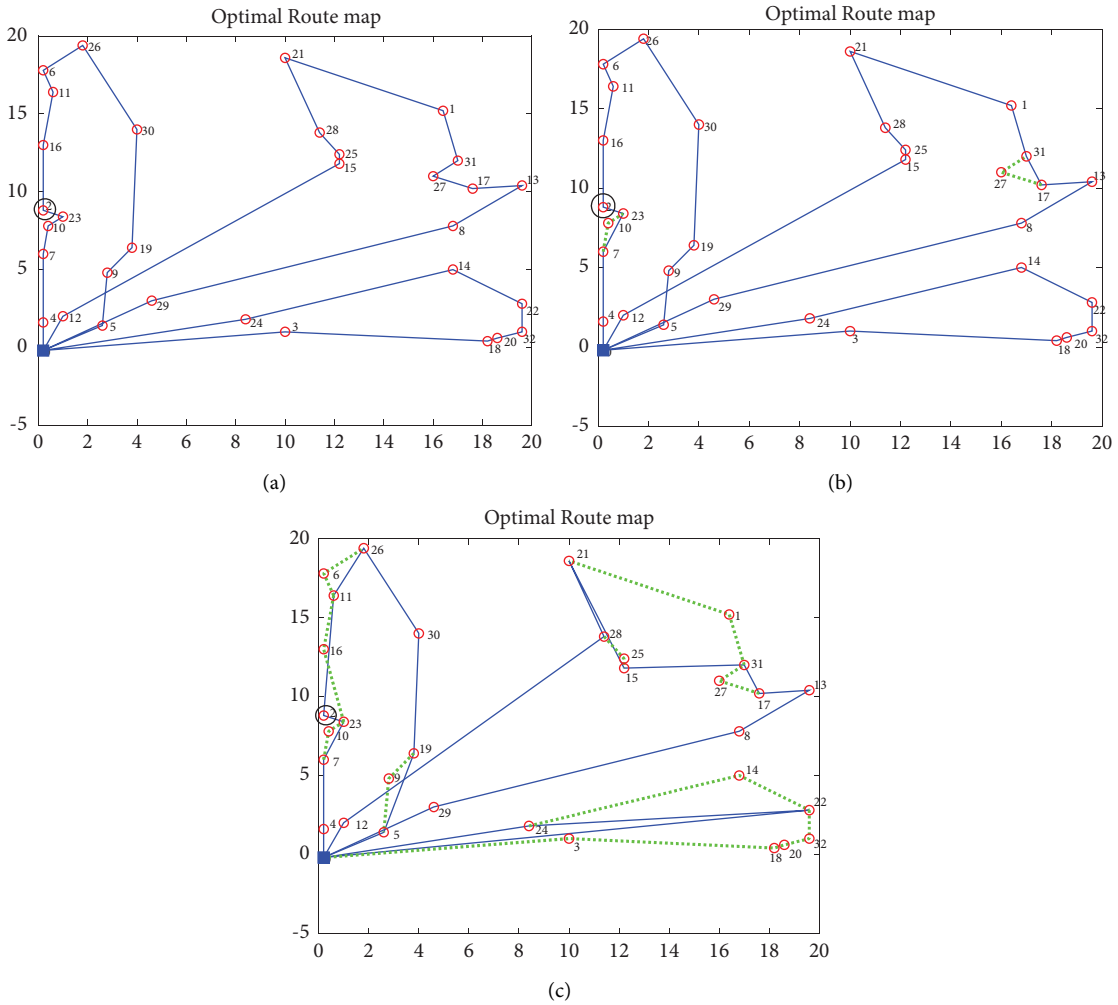

Figure 8: Optimal routing diagram of A-n32-k5 under different service modes. (a) Optimal routing in T mode. (b) Optimal routing in SV mode. (c) Optimal routing in MV mode.

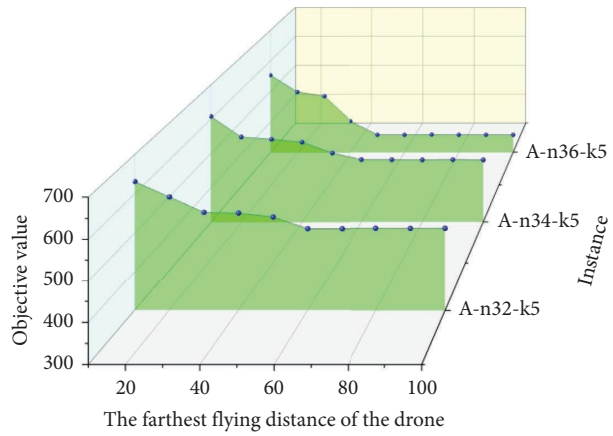

Figure 9: Calculation results for various different farthest flight distances of drone.

service nodes and further reduces the total route cost. However, beyond a certain critical value for the drone capacity and farthest flying distance, the objective function value will not be further reduced. This is because the optimization of one parameter is restricted by other parameters. For example, a maximum loading capacity of 100 kg would enable the drone to serve any customer except those in no-fly zones. Although this would increase the

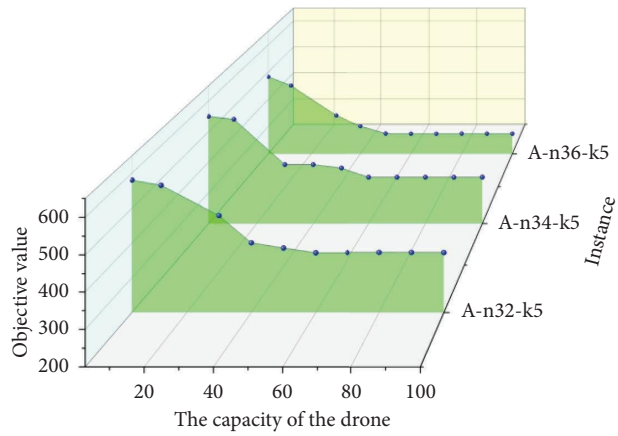

Figure 10: Computational results for different load capacities of drone.

number of customers served, the drone's flight capability and no-fly zones would constrain it. Thus, companies developing logistics drones must consider the flight distance and load capacity, rather than solely pursuing unilateral optimization of either the flight distance or load capacity.

6. Conclusions

This study examines an integrated system that combines trucks and drones for simultaneous pickup and delivery operations while accounting for no-fly zones. This represents an important expansion of the DVRPSPD as the system simultaneously considers constraints such as multivisit, farthest flying distance, maximum loading capacity, no-fly zones, and truck-drone collaboration. We formulate a MILP model with the objective of minimizing the total route cost for both trucks and drones. To address large-scale problems, we develop a two-stage heuristic algorithm comprising two main components: a SA algorithm to tackle the VRPSPD problem and a heuristic approach to handle the DVRPSPD problem with consideration for no-fly zones. In the latter part, we introduce a multidimensional array to represent the collaborative delivery path involving multiple trucks and drones. Additionally, we propose a scheme for adjusting infeasible solutions and an algorithm acceleration strategy for handling no-fly zones. Furthermore, we conduct a series of computational experiments to validate the efficacy of our proposed model and algorithm. Based on the experimental outcomes, as compared to pure truck-based services and the single-visit service mode, the multivisit service mode achieves an average route cost reduction of approximately 13.27% and 12.83%, respectively. While higher payload capacity and increased flight distances confer substantial cost advantages, it is important for enterprises to not solely pursue one-sided optimization. Instead, a balanced consideration of flight distance and payload should be employed to achieve optimal results. In conclusion, this study recommends that logistics enterprises should not only focus on cost reduction and efficiency enhancement through route optimization but also consider the feasibility of flexible and effective distribution vehicles and resource allocation.

To enhance the quality of pickup and delivery services, future research should investigate the incorporation of customer service time constraints. Moreover, deploying multiple drones to provide more efficient service is a promising avenue for expansion. Finally, it is imperative to address the MDVRPSPDNF challenges in low-carbon logistics.

Data Availability

The data in this article can be obtained from VRP Web (dorronsoro.es).

Conflicts of Interest

The authors declare that there are no conflicts of interest.

Acknowledgments

This research was funded by the National Natural Science Foundation of China, grant no. 70431003.

References

[1] N. Boysen, S. Fedtke, and S. Schwerdfeger, "Last-mile delivery concepts: a survey from an operational research perspective," *Spectrum*, vol. 43, pp. 1–58, 2021.

[2] ShenZhen, "Low-altitude Economic Development in ShenZhen Is Accelerating," 2021, https://baijiahao.baidu.com/s?id=1743179880205866376&wfr=spider&for=pc/.

[3] S. J. Kim, G. J. Lim, J. Cho, and M. J. Côté, "Drone-aided healthcare services for patients with chronic diseases in rural areas," *Journal of Intelligent and Robotic Systems*, vol. 88, no. 1, pp. 163–180, 2017.

[4] A. M. Ham, "Integrated scheduling of m-truck, m-drone, and m-depot constrained by time-window, drop-pickup, and m-visit using constraint programming," *Transportation Research Part C: Emerging Technologies*, vol. 91, pp. 1–14, 2018.

[5] J. Wikarek, P. Sitek, and L. Zawarczyn, "An integer programming model for the capacitated vehicle routing problem with drones," in *Proceedings of the International Conference on Computational Collective Intelligence*, pp. 511–520, New York, NY, USA, December 2019.

[6] C. C. Murray and A. G. Chu, "The flying sidekick traveling salesman problem: optimization of drone-assisted parcel delivery," *Transportation Research Part C: Emerging Technologies*, vol. 54, pp. 86–109, 2015.

[7] Q. M. Ha, Y. Deville, Q. D. Pham, and M. H. Hà, "On the min-cost traveling salesman problem with drone," *Transportation Research Part C: Emerging Technologies*, vol. 86, pp. 597–621, 2018.

[8] N. Agatz, P. Bouman, and M. Schmidt, "Optimization approaches for the traveling salesman problem with drone," *Transportation Science*, vol. 52, no. 4, pp. 965–981, 2018.

[9] P. Kitjacharoenchai, M. Ventresca, M. Moshref, S. Lee, J. Tanchoco, and P. Brunese, "Multiple traveling salesman problem with drones: mathematical model and heuristic approach," *Computers & Industrial Engineering*, vol. 129, pp. 14–30, 2019.

[10] P. L. Gonzalez, M. Calle, J. M. Blanco, D. Canca, and J. Andrade, "Truck-drone team logistics: a heuristic approach to multi-drop route planning," *Transportation Research Part C: Emerging Technologies*, vol. 114, pp. 657–680, 2020.

[11] X. Wang, S. Poikonen, and B. Golden, "The vehicle routing problem with drones: several worst-case results," *Optimization Letters*, vol. 11, no. 4, pp. 679–697, 2017.

[12] M. A. Masmoudi, S. Mancini, and R. Baldacci, "Vehicle routing problems with drones equipped with multipackage payload compartments," *Transportation Research Part E: Logistics and Transportation Review*, vol. 164, 2022.

[13] M. W. Ulmer and B. W. Thomas, "Same-day delivery with heterogeneous fleets of drones and vehicles," *Networks*, vol. 72, no. 4, pp. 475–505, 2018.

[14] S. Zhang and L. Li, "The multi-visits drone-vehicle routing problem with simultaneous pickup and delivery service," *Journal of the Operations Research Society of China*, vol. 20, 2023.

[15] S. Meng, X. Guo, D. Li, and G. Liu, "The multi-visit drone routing problem for pickup and delivery services," *Transportation Research Part E: Logistics and Transportation Review*, vol. 169, Article ID 102990, 2023.

[16] A. Otto, N. Agatz, J. Campbell, B. Golden, and E. Pesch, "Optimization approaches for civil applications of unmanned aerial vehicles (uavs) or aerial drones: a survey," *Networks*, vol. 72, no. 4, pp. 411–458, 2018.

[17] I. Khoufi, A. Laouiti, and C. Adjih, "A survey of recent extended variants of the traveling salesman and vehicle routing problems for unmanned aerial vehicles," *Drones*, vol. 3, p. 66, 2019.

[18] G. Macrina, L. Di Puglia Pugliese, F. Guerriero, and G. Laporte, "Drone-aided routing: a literature review," *Transportation Research Part C: Emerging Technologies*, vol. 120, Article ID 102762, 2020.

[19] B. Madani and M. Ndiaye, "Hybrid truck-drone delivery systems: a systematic literature review," *IEEE Access*, vol. 10, pp. 92854–92878, 2022.

[20] M. Marinelli, L. Caggiani, M. Ottomanelli, and M. Dell'Orco, "En route truck-drone parcel delivery for optimal vehicle routing strategies," *IET Intelligent Transport Systems*, vol. 12, no. 4, pp. 253–261, 2018.

[21] Y. Chang and H. Lee, "Optimal delivery routing with wider drone-delivery areas along a shorter truck-route," *Expert Systems with Applications*, vol. 104, pp. 307–317, 2018.

[22] E. Es Yurek and H. Ozmutlu, "A decomposition-based iterative optimization algorithm for traveling salesman problem with drone," *Transportation Research Part C: Emerging Technologies*, vol. 91, pp. 249–262, 2018.

[23] S. Kim and I. Moon, "Traveling salesman problem with a drone station," *IEEE Transactions on Systems, Man, and Cybernetics: Systems*, vol. 49, no. 1, pp. 42–52, 2019.

[24] K. Wang, B. Yuan, M. Zhao, and Y. Lu, "Cooperative route planning for the drone and truck in delivery services: a bi-objective optimisation approach," *Journal of the Operational Research Society*, vol. 71, no. 10, pp. 1657–1674, 2019.

[25] R. Roberti and M. Ruthmair, "Exact methods for the traveling salesman problem with drone," *Transportation Science*, vol. 55, no. 2, pp. 315–335, 2021.

[26] M. Dell'Amico, R. Montemanni, and S. Novellani, "Exact models for the flying sidekick traveling salesman problem," *International Transactions in Operational Research*, vol. 29, no. 3, pp. 1360–1393, 2022.

[27] M. Boccia, A. Masone, A. Sforza, and C. Sterle, "A column-and-row generation approach for the flying sidekick travelling salesman problem," *Transportation Research Part C: Emerging Technologies*, vol. 124, Article ID 102913, 2021.

[28] A. Bogyrbayeva, T. Yoon, H. Ko, S. Lim, H. Yun, and C. Kwon, "A deep reinforcement learning approach for solving the traveling salesman problem with drone," *Transportation Research Part C: Emerging Technologies*, vol. 148, Article ID 103981, 2023.

[29] M. Lin, Y. Chen, R. Han, and Y. Chen, "Discrete optimization on truck-drone collaborative transportation system for delivering medical resources," *Discrete Dynamics in Nature and Society*, vol. 2022, Article ID 1811288, 13 pages, 2022.

[30] S. Mahmoudinazlou and C. Kwon, "A hybrid genetic algorithm with type-aware chromosomes for traveling salesman problems with drone," *Neural and Evolutionary Computing*, vol. 15, 2023.

[31] R. Raj and C. C. Murray, "The multiple flying sidekicks traveling salesman problem with variable drone speeds," *Transportation Research Part C: Emerging Technologies*, vol. 120, Article ID 102813, 2020.

[32] K. Peng, J. Du, F. Lu et al., "A hybrid genetic algorithm on routing and scheduling for vehicle-assisted multi-drone parcel delivery," *IEEE Access*, vol. 7, pp. 49191–49200, 2019.

[33] J. Freitas and P. Penna, "A variable neighborhood search for flying sidekick traveling salesman problem," *International Transactions in Operational Research*, vol. 27, pp. 267–290, 2020.

[34] M. Dell'Amico, R. Montemanni, and S. Novellani, "Modeling the flying sidekick traveling salesman problem with multiple drones," *Networks*, vol. 78, no. 3, pp. 303–327, 2021.

[35] S. Cavani, M. Iori, and R. Roberti, "Exact methods for the traveling salesman problem with multiple drones," *Transportation Research Part C: Emerging Technologies*, vol. 130, Article ID 103280, 2021.

[36] S. Lu, R. Kuo, Y. Ho, and A. T. Nguyen, "Improving the efficiency of last-mile delivery with the flexible drones traveling salesman problem," *Expert Systems with Applications*, vol. 209, Article ID 118351, 2022.

[37] G. Tiniç, O. Karasan, B. Kara, J. F. Campbell, and A. Ozel, "Exact solution approaches for the minimum total cost traveling salesman problem with multiple drones," *Transportation Research Part B: Methodological*, vol. 168, pp. 81–123, 2023.

[38] Z. Luo, M. Poon, Z. Zhang, Z. Liu, and A. Lim, "The multi-visit traveling salesman problem with multi-drones," *Transportation Research Part C: Emerging Technologies*, vol. 128, Article ID 103172, 2021.

[39] S. T. Windras Mara, A. Rifai, and B. Sopha, "An adaptive large neighborhood search heuristic for the flying sidekick traveling salesman problem with multiple drops," *Expert Systems with Applications*, vol. 205, Article ID 117647, 2022.

[40] B. Mahmoudi and K. Eshghi, "Energy-constrained multi-visit tsp with multiple drones considering non-customer rendezvous locations," *Expert Systems with Applications*, vol. 210, Article ID 118479, 2022.

[41] Z. Wang and J. Sheu, "Vehicle routing problem with drones," *Transportation Research Part B: Methodological*, vol. 122, pp. 350–364, 2019.

[42] F. Tamke and U. Buscher, "A branch-and-cut algorithm for the vehicle routing problem with drones," *Transportation Research Part B: Methodological*, vol. 144, pp. 174–203, 2021.

[43] L. Zhen, J. Gao, Z. Tan, S. Wang, and R. Baldacci, "Branch price-and-cut for trucks and drones cooperative delivery," *IISE Transactions*, vol. 55, no. 3, pp. 271–287, 2023.

[44] J. Euchi and A. Sadok, "Hybrid genetic-sweep algorithm to solve the vehicle routing problem with drones," *Physical Communication*, vol. 44, Article ID 101236, 2021.

[45] D. Lei, Z. Cui, and M. Li, "A dynamical artificial bee colony for vehicle routing problem with drones," *Engineering Applications of Artificial Intelligence*, vol. 107, Article ID 104510, 2022.

[46] D. Schermer, M. Moeini, and O. Wendt, "A matheuristic for the vehicle routing problem with drones and its variants," *Transportation Research Part C: Emerging Technologies*, vol. 106, pp. 166–204, 2019.

[47] R. Kuo, E. Edbert, F. Zulvia, and S. H. Lu, "Applying nsga-ii to vehicle routing problem with drones considering makespan and carbon emission," *Expert Systems with Applications*, vol. 221, Article ID 119777, 2023.

[48] R. Kuo, S. Lu, P. Lai, and S. T. W. Mara, "Vehicle routing problem with drones considering time windows," *Expert Systems with Applications*, vol. 191, Article ID 116264, 2022.

[49] I. Dayarian, M. Savelsbergh, and J. Clarke, "Same-day delivery with drone resupply," *Transportation Science*, vol. 54, no. 1, pp. 229–249, 2020.

[50] Y. Lu, C. Yang, and J. Yang, "A multi-objective humanitarian pickup and delivery vehicle routing problem with drones," *Annals of Operations Research*, vol. 319, pp. 291–353, 2022.

[51] H. Jeong, B. Song, and S. Lee, "Truck-Drone hybrid delivery routing: payload-energy dependency and no-fly zones," *International Journal of Production Economics*, vol. 214, pp. 220–233, 2019.

[52] N. K. Yu, W. Jiang, R. Hu, B. Qian, and L. Wang, "Learning whale optimization algorithm for open vehicle routing problem with loading constraints," *Discrete Dynamics in Nature and Society*, vol. 2021, Article ID 8016356, 14 pages, 2021.

[53] Z. Q. Liu, Y. P. Chen, J. Li, and D. Zhang, "Spatiotemporal-dependent vehicle routing problem considering carbon emissions," *Discrete Dynamics in Nature and Society*, vol. 2021, Article ID 9729784, 21 pages, 2021.

[54] J. F. Campbell, D. C. Sweeney, and J. Zhang, "Strategic Design for Delivery with Linked Transportation Assets: Trucks and Drones," *Technical Report Midwest Transportation Center*, vol. 71, 2018.

[55] U. A. V. ShunFeng, "An unmanned aerial vehicle," 2018, https://dan.com/buy-domain/sf-tech.com?redirected=true.

[56] X. L. Wan and H. Z. Wang, "Efficient semi-external depth-first search," *Information Sciences*, vol. 599, pp. 170–191, 2022.